

# **Dynamic Modeling and Analysis of an Olympic Curling Shot**

**ME-200, Prof. Rosen  
The Cooper Union  
12/15/2023**

**Joon Kim**

## I. Problem

The physics behind the interactions of curling stones on ice in curling gameplay holds immense intrigue and practical importance for optimizing outcomes. For example, one such example is in the way players line up their shots to best take advantage of collision physics. They often draw planning diagrams that predict the motion of the shooting stone, as well as all other stones on the field, to best optimize their gameplay. It is evident, then, that players take advantage of physics on the field to great extent, thus prompting this dynamical study.

This project centers on a clip from the gold medal match in the 2018 PyeongChang Olympics [1], depicting a scenario where one curling stone sets off a series of consequential interactions among other stones. These interactions lead to distinct collisions, influencing the final positions and velocities of the stones involved. The aim is to analyze the momentum and collision mechanics to model these interactions and understand their effects on the stones' trajectories and placements. A secondary objective is to experimentally determine the material properties of curling gameplay: the coefficient of restitution between two stones, and the average friction of the rink.

To achieve these objectives, this study will make use of Tracker, a video motion-tracking system, and Python coding, along with the mathematical principles associated with collisions and motion, to ultimately model the intricate interactions of curling stones and the physics that govern this game.

## II. Approach

### A. Assumptions and Simplifications

In developing a model to simulate the interactions among curling stones, several simplifications and assumptions are made to reduce the complexity of the system for a manageable analysis while aiming to retain its fundamental dynamics. These assumptions and simplifications aim to strike a balance between accuracy and feasibility in the analysis.

#### 1. Geometry of Curling Stones

The curling stones, while inherently three-dimensional cylindrical objects, are analyzed in a two-dimensional context. They are simplified to be the projection of a perfectly circular cylinder onto the xy plane, allowing for easier examination of their movements from an overhead view. This representation is justified because the band at which the stones collide is the widest segment.

#### 2. Constant, Small Frictional Force on the Ice

It is assumed that the frictional force between the curling stones and rink remains constant and small throughout the simulation. This assumption is supported by the selected video, where there is no evidence of sweeping, indicating minimal surface variations within the circular sections of the curling lanes. Additionally, because the nonconservative work done by friction is a function of path length, friction is assumed to be negligible for most short-term interactions.

#### 3. Neglect of Air Drag

Air resistance acting on the moving stones is disregarded. The stones' motion consists of only relatively slow velocities and short distances during their movement across the lane. Considering that drag force is a function of velocity, and the stones' movement is not prolonged, the impact of air resistance is deemed negligible for this analysis.

#### 4. Assumption of Center of Mass (COM) Location

It is assumed that the center of mass of each curling stone coincides with the center of the granite disc. Although the stone features a handle on top, this handle, constructed from a less dense material, is relatively small compared to the stone itself. Thus, the center of mass in the xy plane is simply the center of the projected circle, which simplifies the assessment of its motion and interactions.

#### 5. Utilization of Coefficient of Restitution

The coefficient of restitution will be utilized to model stone-to-stone collisions. Because the coefficient of restitution is a material constant, it is assumed to remain constant for all standard curling stones, and thus across all interactions simulated.

### B. Tracker and Obtaining Data

Note that all Python graphs displaying the initial data gathered from Tracker can be viewed in *Appendix A*.

The video clip [1] was imported into Tracker. In the video, the camera reference frame moves and zooms out, meaning that both position and scale of the video frame were changing with time. To remedy this, the center, as well as top-edge and right-edge of the largest field circle were tracked as particles. The origin was then affixed to the center, with calibration sticks of length 1.829m (the radius of the outer circle [2]) affixed to the tracked edges, as displayed in "Fig. B.1" of *Appendix B*. Thus, an axis was created such that its origin and scale would evolve with the camera position and would be fixed on real-world elements for accuracy.

The position of each stone (marked A, B, and C as shown in "Fig. B.2," *Appendix B*), was then tracked using its center of mass. The data of each stone, containing time, x, and y displacement, was exported for further analysis in Python.

To analyze angular motion, new axes were set with their origins placed at the (previously tracked) centers of masses, as displayed in "Fig. B.3" in *Appendix B*. This way, as the stones moved in-frame, the axes would reposition themselves upon the stones accordingly. With the central axes set, a point on the edge of each stone was chosen. Its angular motion was tracked with respect to the centroidal origin, and the datafiles of angle vs. time were exported per stone.

To find the angular and linear velocities of each stone, pre- and post-collision, the datafiles were imported into Python (see scripts "ABC\_Motion.py" and "ABC\_Angular.py"), and periods of time were split using the times of collision, or just by eye for those without a well-defined "end-time." A period long enough to find an average velocity, yet short enough to avoid decay due to friction, was estimated. Then, the finite Riemann Sum was approximated per dataset to find a series of instantaneous velocities. The mean of these instantaneous velocities was taken, per chunk of time, to find suitable values of velocity before and after each collision.

To estimate the coefficient of restitution, Collision 1 (consisting of A hitting B) was isolated. A new axis was made with its origin at the combined center of mass of the two stones. Its normal axis was rotated to intersect the two separate centroids of the stones at the time of collision. Thus, its tangential axis was simply tangent to the point of contact between the two stones. This axis can be viewed in “Fig. B.4” in *Appendix B*. The velocities were automatically split into components, with the basis set of  $\{\hat{n}, \hat{t}\}$ , and exported to Python. The coefficient of restitution was calculated as such, using average velocity as discussed previously. This calculation can be found in script “COR.py.”

$$e = \frac{\mathbf{v}_{Bt}' - \mathbf{v}_{At}'}{\mathbf{v}_{At} - \mathbf{v}_{Bt}}$$

It should be noted that although the system center of mass *does* move with respect to time, and thus the measured velocities of A and B are with respect to this moving frame, the coefficient of restitution is based only on the relative velocities of approach and separation, so the calculation works as described. Stones A and B still move, with respect to the moving origin, the same overall amount since that origin is always based on their positions.

Finally, the average coefficient of kinetic friction was estimated by isolating the movement of Stone A after its first collision, until its eventual rest (see “Fig. B.5,” *Appendix B*). Because its instantaneous velocity after the collision (at  $t=1.120\text{s}$ ) was found above, the time at which it came to rest ( $t=5.520\text{s}$ ) allowed for a calculation of required acceleration, and thus average frictional force, to satisfy this movement, using the following equations:

$$F_f = \mu N = \mu mg = ma \Rightarrow a = \mu g$$

$$v_f = v_i + a\Delta t \Rightarrow 0 = v_i + \mu g \Delta t$$

$$\mu = -\frac{v_i}{g\Delta t}, \quad g = -9.81 \text{ m/s}^2$$

### C. Mode of Analysis & Equations of Motion

The overarching lens of analysis for this procedure will be of an oblique central impact, which occurs at both collisions. The impulse-momentum diagram for Collision 1 specifically is shown below (though the same diagram can be applied for Collision 2). Note that the velocities shown are those of the point of contact, as Stones A and B are rigid bodies, and that Stone B starts at rest.

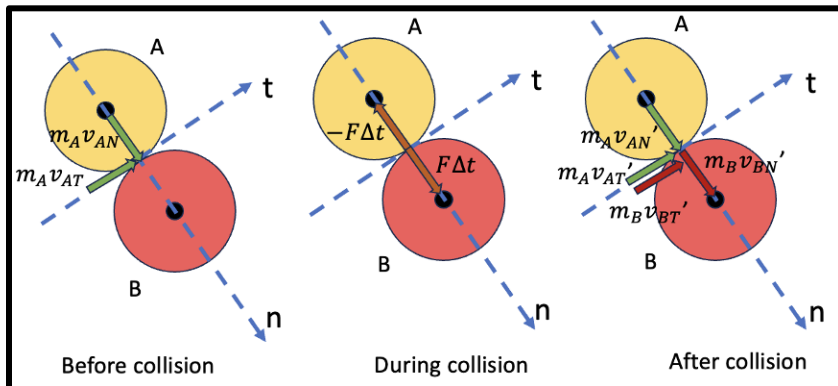


**Figure 1. Impulse-momentum diagram (in n-t axes) for Collision 1 (A-B).**

Because the momenta of the system will be analyzed as a whole, the impulsive force shown during collision can be neglected, as it will be resolved as an internal force. There is an assumption that no other external impulses are applied. The equations of motion that follow from the diagram above are as such:

Along the tangential axes, velocity is conserved because there is no impulse whatsoever:

$$\vec{v}_{At} = \vec{v}'_{At}; \quad \vec{v}_{Bt} = \vec{v}'_{Bt} = 0$$

Along the normal axes, there is conservation of momentum. Note however that the masses of both stones are equal, and therefore can be factored out.

$$\begin{aligned} mv_{An} + mv_{Bn} &= mv'_{An} + mv'_{Bn} \\ v_{An} &= v'_{An} + v'_{Bn} \end{aligned}$$

Additionally, along the normal, the previously found coefficient of restitution can be used:

$$\begin{aligned} v'_{Bn} - v'_{An} &= e(v_{An} - v_{Bn}) \\ v'_{Bn} &= v'_{An} + e(v_{An}) \end{aligned}$$

At this point, it should be noted that because the stones are rigid bodies that rotate while translating (rotating while slipping), the tracked velocities of the center of mass must first be converted to velocities at the edges of the stones (the point of contact). Let A denote the point of contact, and G denote the center of mass.

$$\vec{v}_A = \vec{v}_G + (\vec{\omega} \times \vec{r}_{A/G})$$

Resolving the velocity of point A into components gives the following. Note that these velocities are the ones used in the collision-calculations.

$$\vec{v}_{An} = \vec{v}_{Gn}; \quad \vec{v}_{At} = \vec{v}_{Gt} + r\vec{\omega}\hat{t}$$

After the collision calculations, the final velocities obtained are once again those of the point of contact. Thus, it becomes necessary to convert those velocities into the centroidal velocities again:

$$\vec{v}_{Gt} = \vec{v}_{At} - r\vec{\omega}\hat{t}$$

However, this meant that a relationship between initial and final angular velocities needed to be found, as the unknown value of  $\vec{v}_{Gt}'$  meant that there was no solvable relationship between linear velocity and angular velocity, without external information.

Conservation of angular momentum was attempted below; although the sum of total system momenta could be found, there was no way to determine the values of  $\omega'_A$  and  $\omega'_B$ , specifically without already knowing the value of  $\vec{v}_{Gt}'$ .

$$I\omega_A + I\omega_B = I\omega'_A + I\omega'_B$$

Another attempt to determine the angular velocity was finding the impulsive torque exerted by one stone on another when they collide, that the angular velocity could be found, as shown below. However, it was soon realized that because the impulsive torque is that of friction and is dependent on the normal force, this force changes with every collision, and only introduces more unknown variables that could not be resolved without extra information.

$$I\omega_A + M\Delta t = I\omega'_A$$

$$M = F_f r = \mu N r$$

Thus, because the unknown variables were dependent only on each other, it was quickly realized that the system was under-determined. Although the hope was to complete a simulation

with only initial positions and velocities, two additional pieces of information were added in order to properly constrain the system: the post-collision angular velocities of stone A and C.

## D. Python Simulation

### a. Rigid-Body Analysis

For the modeling done below, the initial positions of all stones, the starting angular and linear velocity of stone A, and the post-collision angular velocities of stone A and C, were all introduced as initial conditions.

To model oblique central impact, the normal and tangential components of the velocity need to be calculated. The geometry of the stones being circles, a normal vector that intersects the point of collision can be calculated by taking the points of the centers of mass of the two stones. Let the position of stones A and B be denoted by the points A and B, respectively.

$$\vec{v}_{A,n}(x,y) = (B_{CoM,x} - A_{CoM,x}) \hat{i} + (B_{CoM,y} - A_{CoM,y}) \hat{j}$$

This vector, when divided by its own magnitude, will serve as the unit normal vector, which will be used in a dot product with the initial velocity to determine the magnitude of the normal component of the initial velocity.

$$\hat{n}(x,y) = \frac{\vec{v}_{A,n}}{|\vec{v}_{A,n}|} = \frac{(B_{CoM,x} - A_{CoM,x}) \hat{i} + (B_{CoM,y} - A_{CoM,y}) \hat{j}}{\sqrt{(B_{CoM,x} - A_{CoM,x})^2 + (B_{CoM,y} - A_{CoM,y})^2}}$$

With this newly calculated normal velocity, the tangential component of the same initial velocity can be calculated using the equation below:

$$\vec{V}_A = \vec{v}_{A,n} + \vec{v}_{A,t} \Rightarrow \vec{v}_{A,t} = \vec{v}_A - \vec{v}_{A,n}$$

From the tangential component vector, the unit tangent vector can be derived. This vector will be necessary later for expressing normal-tangential component vectors back into a vector with xy-components.

Now that the velocities have been split to normal and tangential components (keep in mind that the initial velocity of the stone getting hit is zero), the next step is to solve the system of equations of oblique central impact consisting of 4 equations and 4 unknowns (see equations of motion above). Keep in mind that stone B is initially at rest.

It is important to take note that the velocities calculated here are velocities based on the point of collision; this implies that to find the velocity on the Center of Mass, angular velocity needs to be considered. The following needs to be applied to the velocities on the collision point to calculate the velocities on the center of mass:

$$\vec{v}_{B,t,G}' = (v_{B,t}' - r\omega_B') \hat{t}$$

The final angular velocities,  $\omega'$ , are calculated using the conservation of angular momentum. After determining the velocity at the center of mass, the velocities are calculated to be in terms of the x-y coordinate system, which is done by multiplying the magnitude of the normal-tangential components with its respective unit vectors and adding appropriate vectors to one another. This is essential for the final velocities of the first collision as the normal-tangential axis will be different and change for the second collision.

$$\vec{V}_B(x,y) = \{v_{B,n}' \cdot \hat{n}_x + (\vec{v}_{B,t}' - r\omega_B') \hat{t}_x\} \hat{i} + \{v_{B,n}' \cdot \hat{n}_y + (\vec{v}_{B,t}' - r\omega_B') \hat{t}_y\} \hat{j}$$

With the calculated final velocity of stone B, a parametrized equation was made using the velocity in addition to position vectors representing the path stone B takes after the first collision.

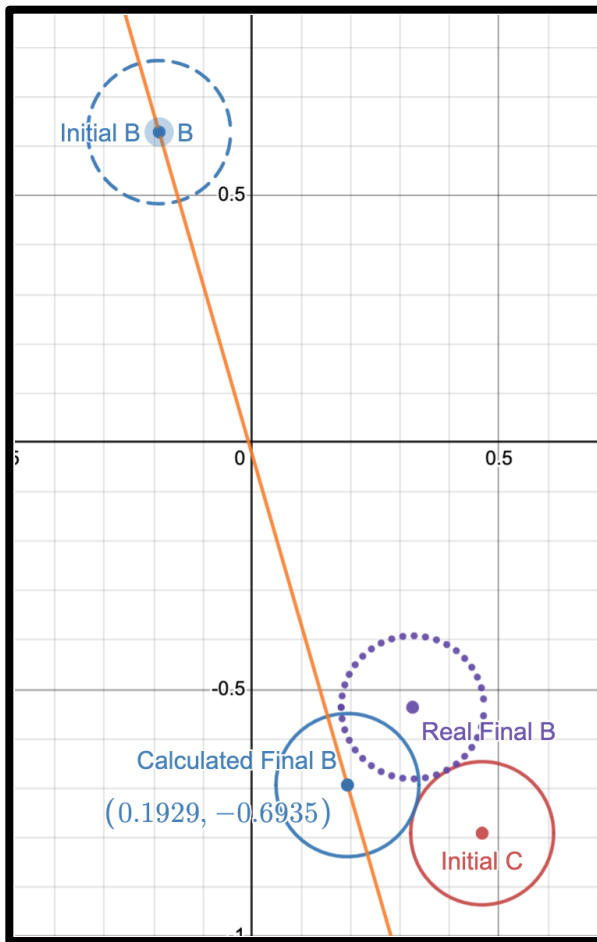


**Figure 2. Trajectory of Stone B after Collision 1 in Rigid Body Analysis (in x-y axes)**

Though it is a bit off the real tracker data location, the stone B travels a path that leads to a second collision. Calculating the second collision of stone B and stone C will consist of the same process and the utilization of the same python code with changed initial conditions.

### b. Point-Mass Assumption

When analyzing the angular motion of the curling stones derived from tracker, it becomes noticeable the angular velocities do not obey the conservation of angular momentum under the assumption of zero external torque. After collision 1 between stone A and B, the angular velocity of both stones somehow increases (see *Table 2:* ). The result implies that there must be some external source of torque. This may be due to an unpredictable torque from uneven ice on the floor leading to friction causing an irregular angular motion on the curling stones.

To account for this, an alternative python model was created where the angular velocity was neglected, and the stones were treated more like point masses than rigid bodies. That means in the script, the final angular velocities were not calculated nor considered in the calculation of the final velocities, thus:

$$\vec{V}_B(x,y) = \{v'_{B,n} \cdot \hat{n}_x + v'_{B,t} \hat{t}_x\} \hat{i} + \{v'_{B,n} \cdot \hat{n}_y + v'_{B,t} \hat{t}_y\} \hat{j}$$

Once again, the path stone B takes after the first collision is calculated using a parametrized equation derived from the calculated final velocity along with position vectors.

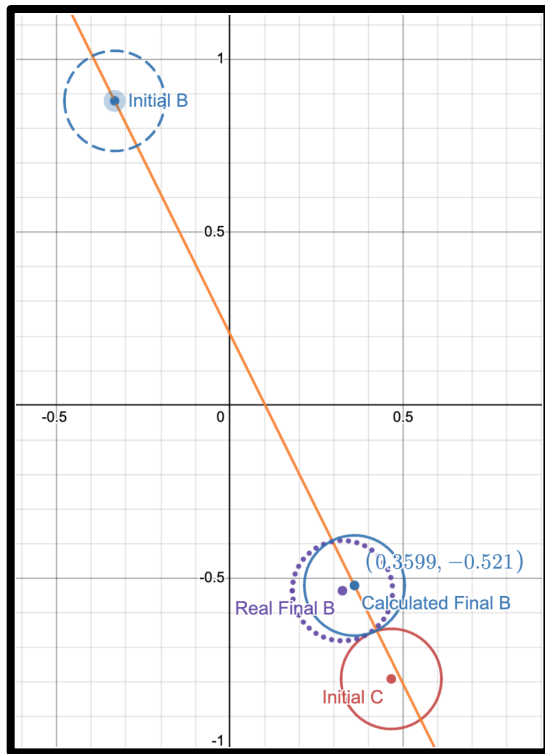


**Figure 3. Trajectory of Stone B after Collision 1 with Point Mass Assumption (in x-y axes)**

When comparing “Figure 3” to “Figure 2” (as well as *Table 2* and *Table 4*, found in *Appendix A*), neglecting the angular motion of the stones result in a more accurate model of what happens in real life. Thus, further deemphasizing the significance of the stones’ angular motion to its linear motion.

### III. Results and Discussion

“Fig. 4” and “Fig. 5” displayed below provide a comparison between the projected trajectories of Stone B, using Python-calculated values of velocity, to the true path of B as determined in Tracker. Stone B was chosen for this comparison because it was the one stone that was experimentally simulated from start-to-finish, for both Collision 1 and 2.

Very interestingly, the point-mass simplification result is much closer to the true trajectory, in both x and y motion. This is interesting because this simplification of point-mass ignores rotational motion entirely and conflates the velocity of the center of mass with the velocity of point of contact for all collisions. This simplification does introduce some error into the final trajectory because, as seen, the plot does not quite match up with the true line either.

However, the rigid-body analysis (though theoretically the more “correct” way to analyze this system) predicts a trajectory that deviates much more extremely from the true trajectory. Not only are the magnitudes of velocity much more different, but after Collision 2 the direction of velocity changes entirely.

These results indicate that the un-accounted for torque within the system produce greater error within the simulations than the erroneous simplification of ignoring rotation entirely.

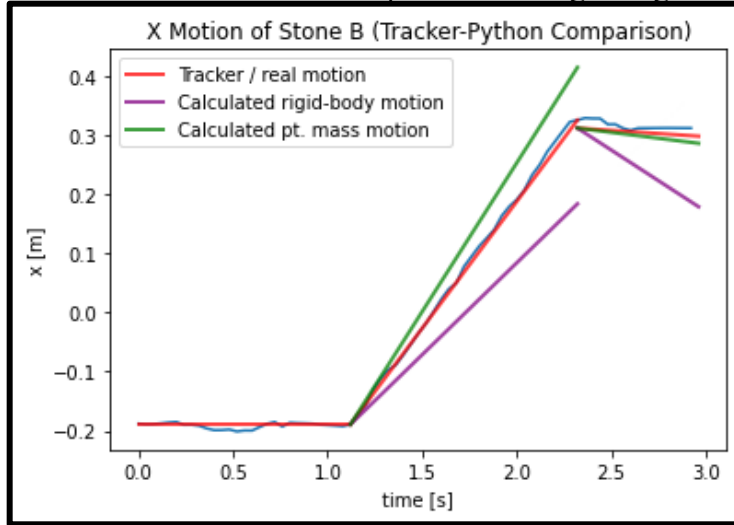


**Figure 4. Comparison of simulated x-motion of Stone B using two modes of Python analysis to the “real” Tracker trajectory.**

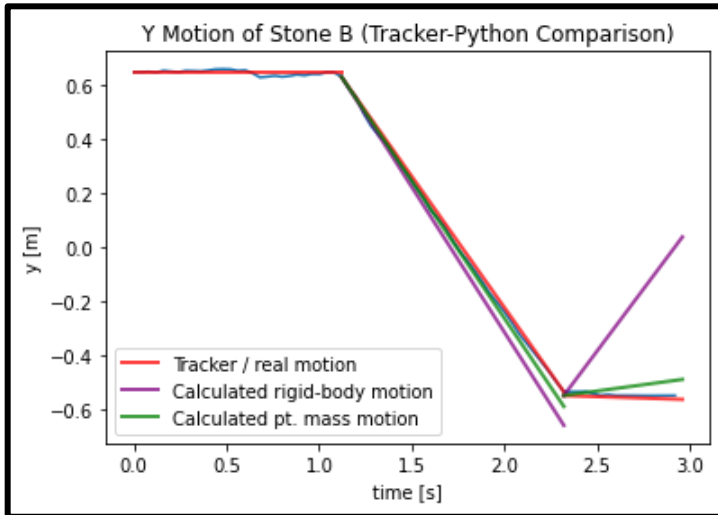


**Figure 5. Comparison of simulated y-motion of Stone B using two modes of Python analysis to the “real” Tracker trajectory.**

Additionally, the calculated values for coefficient of restitution and kinetic friction are displayed below in comparison to accepted literature values [3] [4].

**Table 1. Comparison of experimental material values to actual.**

	Experimental	Actual
<b>Coefficient of Restitution</b>	0.8345	$0.83 \pm 0.06$
<b>Coefficient of Kinetic Friction</b>	0.0109	[0.006, 0.016]

As seen above, the experimental values calculated in this procedure agree with those accepted in scientific literature. Because the coefficient of restitution and friction were calculated using principles of linear motion, this once again suggests that the bulk of the error in the trajectories above are due to unforeseen conditions that mainly affected the angular momenta.

In summation, the assumption of constant friction across the rink was quite glaringly wrong. There must be some sort of uneven distribution of friction that acts on the bottom of each stone to cause an increase in angular momentum after the collisions (as discussed previously). To avoid this problem in the future, an experimental setup should be taken where the surface of the ice can be controlled.

Other sources of error that were probably present, but less significant, include the low framerate of the video, which caused inaccuracies in the Tracker app, as well as the changing camera angle. Though some aspects of the changing video scale were accounted for through the axes setup, warping at the far-edges of the video could not be remedied without an accurate scale to calibrate with. Thus, an ideal experimental setup would also include a high frame-rate camera that remains perpendicular to the rink surface at all times.

## IV. References

- [1] Olympics, "USA vs. SWE - Men's Curling - Full Gold Medal Match | PyeongChang 2018 Replays," Youtube, 1:47:54, [https://www.youtube.com/watch?v=lg3\\_g-pfcLE&t=6456s](https://www.youtube.com/watch?v=lg3_g-pfcLE&t=6456s), (accessed December 15, 2024).
- [2] "The Rules of Curling and Rules of Competition," World Curling Federation, July 2023, [https://s3.eu-west-1.amazonaws.com/media.worldcurling.org/media.worldcurling.org/wcf\\_worldcurling/2023/07/28122449/2023-The-Rules-of-Curling.pdf](https://s3.eu-west-1.amazonaws.com/media.worldcurling.org/media.worldcurling.org/wcf_worldcurling/2023/07/28122449/2023-The-Rules-of-Curling.pdf), (accessed December 15, 2024).
- [3] [1] R. Barnes et al., "Experimental determination of the coefficient of restitution for meter-scale granite spheres," Icarus, <https://www.sciencedirect.com/science/article/pii/S0019103510003465?via%3Dihub#s0040> (accessed Dec. 15, 2023).
- [4] J. Li, S. Li, W. Zhang, B. Wei, and Q. Yang, "Experimental measurement of ice-curling stone friction coefficient based on computer vision technology: A case study of 'ice cube' for 2022 Beijing Winter Olympics," MDPI, <https://www.mdpi.com/2075-4442/10/10/265> (accessed Dec. 15, 2023).

## V. Appendix A

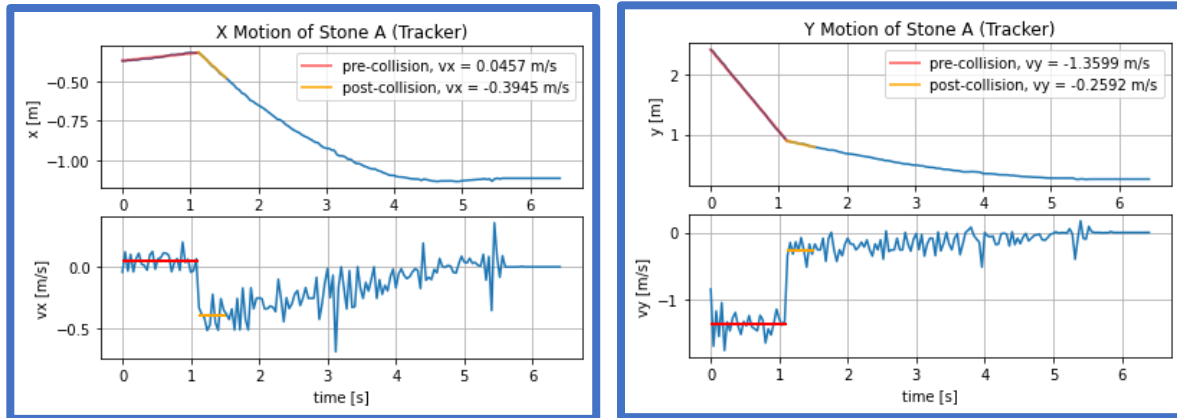


**Figure A.1.** Python-generated plots of Stone A motion, with calculated velocities.

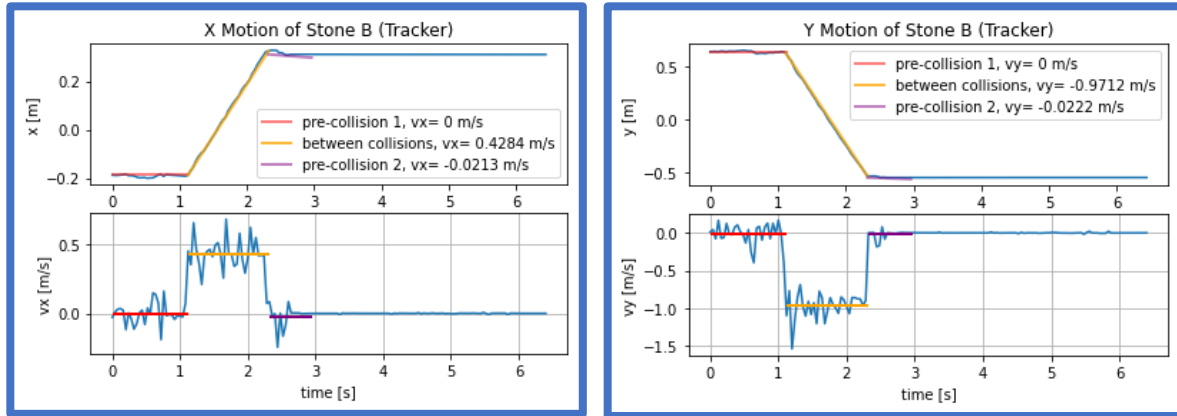


**Figure A.2.** Python-generated plots of Stone B motion, with calculated velocities.

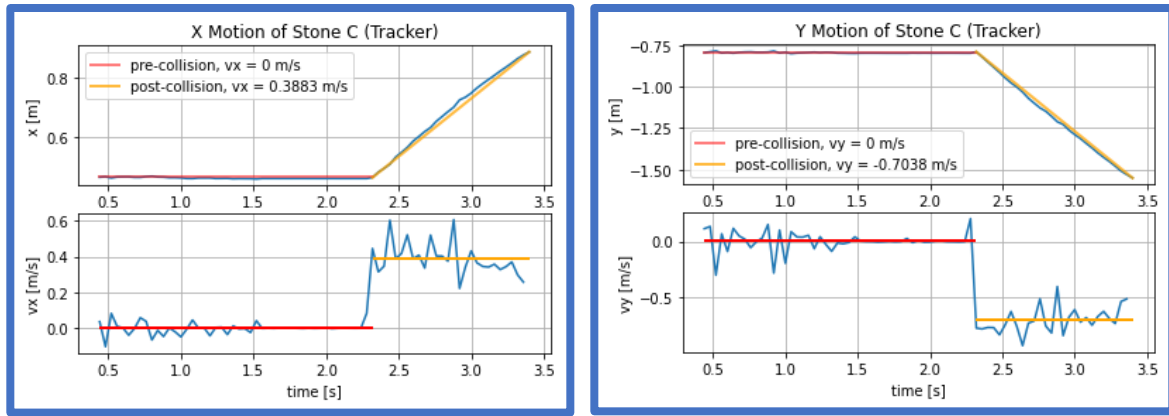


**Figure A.3.** Python-generated plots of Stone C motion, with calculated velocities.

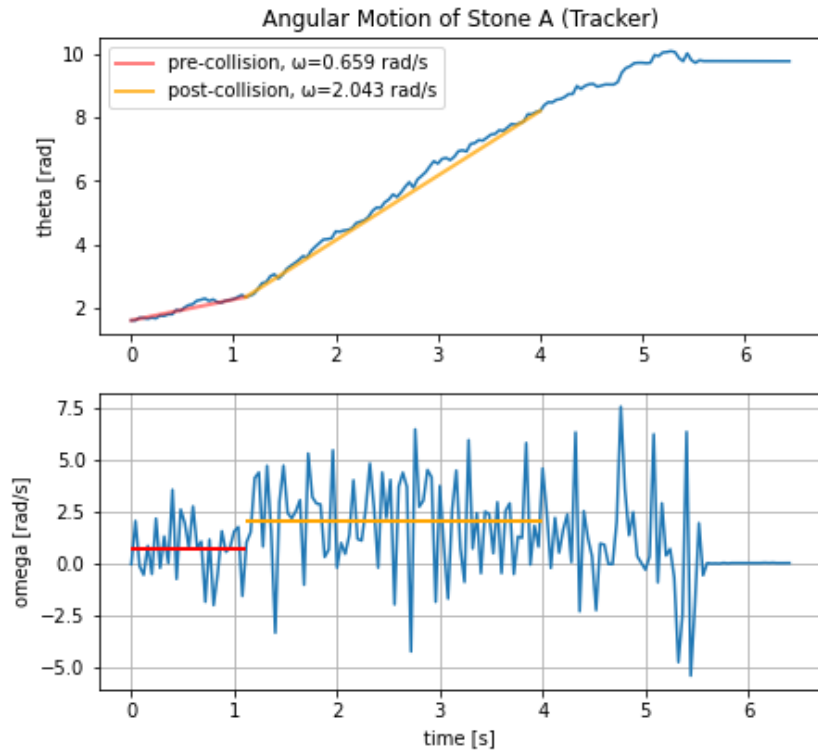


**Figure A.4.** Python-generated plot of Stone A angular motion, with calculated velocities.

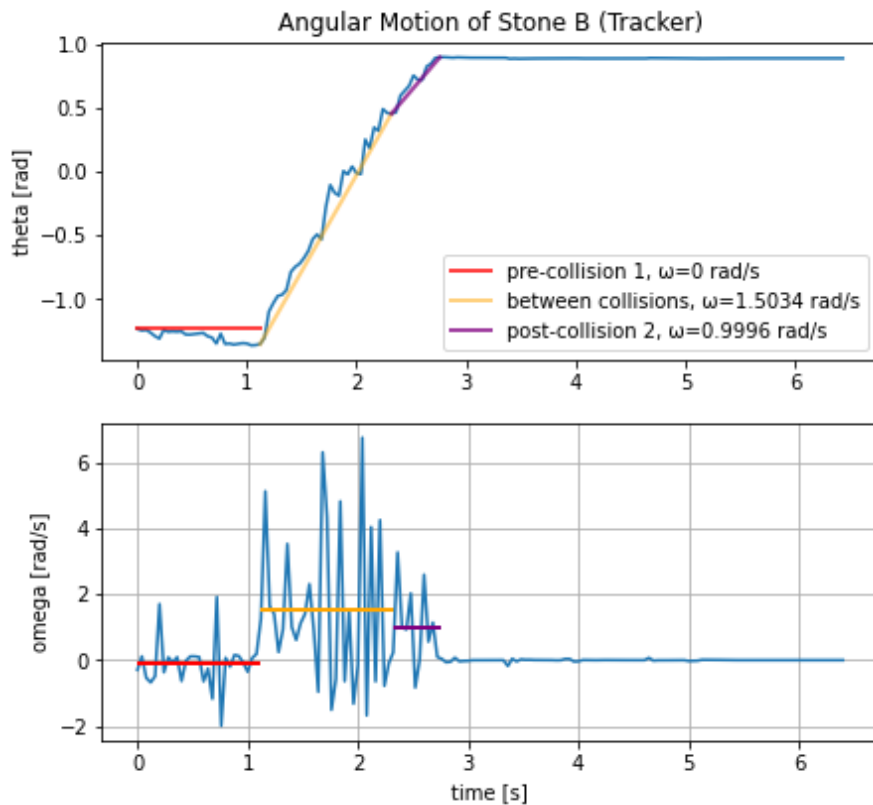


**Figure A.5.** Python-generated plot of Stone B angular motion, with calculated velocities.

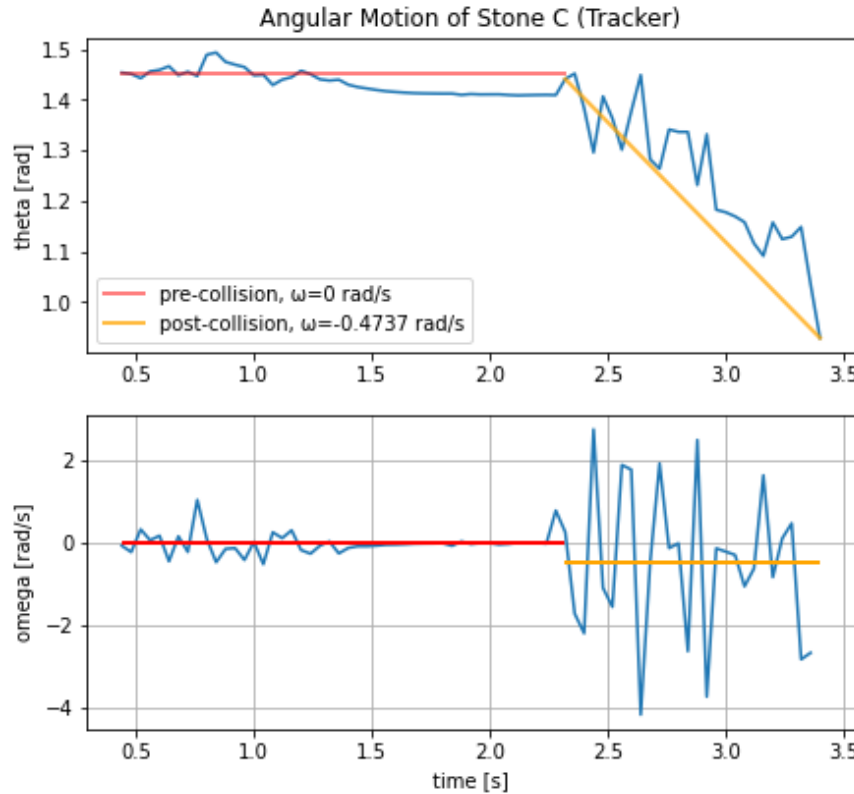


**Figure A.6.** Python-generated plot of Stone C angular motion, with calculated velocities.

**Table 2.** Tracker-Generated Values.

	STONE A			STONE B			STONE C		
	$\vec{r}$ (m)	$\vec{v}$ (m/s)	$\vec{\omega}$ (rad/s)	$\vec{r}$ (m)	$\vec{v}$ (m/s)	$\vec{\omega}$ (rad/s)	$\vec{r}$ (m)	$\vec{v}$ (m/s)	$\vec{\omega}$ (rad/s)
Collision 1 (A+B) Frame 53 $t = 1.120\text{s}$	$-0.320\hat{i} + 0.894\hat{j}$	$0.0457\hat{i} - 1.3599\hat{j}$	$0.6586\hat{k}$	$-0.189\hat{i} + 0.629\hat{j}$	0	0			
Post-Collision 1 (A+B) Frame 54 $t = 1.160\text{s}$	$-0.333\hat{i} + 0.880\hat{j}$	$-0.3945\hat{i} - 0.2592\hat{j}$	$2.0433\hat{k}$	$-0.171\hat{i} + 0.585\hat{j}$	$0.4284\hat{i} - 0.9712\hat{j}$	$1.5034\hat{k}$			
Collision 2 (B+C) Frame 83 $t = 2.320\text{s}$				$0.325\hat{i} - 0.536\hat{j}$	$0.4284\hat{i} - 0.9712\hat{j}$	$1.5034\hat{k}$	$0.466\hat{i} - 0.791\hat{j}$	0	0
Post-Collision 2 (B+C) Frame 84 $t = 2.360\text{s}$				$0.328\hat{i} - 0.536\hat{j}$	$-0.0213\hat{i} - 0.0222\hat{j}$	$0.9996\hat{k}$	$0.484\hat{i} - 0.822\hat{j}$	$0.3883\hat{i} - 0.7038\hat{j}$	$-0.4737\hat{k}$

**Table 3. Python-Calculated Values Using Rigid-Body Analysis.**

	STONE A			STONE B			STONE C		
	$\vec{r}$ (m)	$\vec{v}$ (m/s)	$\vec{\omega}$ (rad/s)	$\vec{r}$ (m)	$\vec{v}$ (m/s)	$\vec{\omega}$ (rad/s)	$\vec{r}$ (m)	$\vec{v}$ (m/s)	$\vec{\omega}$ (rad/s)
Collision 1 (A+B) Frame 53 $t = 1.120\text{s}$	$-0.320\hat{i} + 0.894\hat{j}$	$0.0457\hat{i} - 1.3599\hat{j}$	$0.6586\hat{k}$	$-0.189\hat{i} + 0.629\hat{j}$	0	0			
Post-Collision 1 (A+B) Frame 54 $t = 1.160\text{s}$		$-0.1734\hat{i} - 0.1615\hat{j}$	$2.0433\hat{k}$		$0.3105\hat{i} - 1.075\hat{j}$	$-1.3847\hat{k}$			
Collision 2 (B+C) Frame 83 $t = 2.320\text{s}$				$0.1929\hat{i} - 0.6935\hat{j}$	$0.3105\hat{i} - 1.075\hat{j}$	$-1.3847\hat{k}$	$0.466\hat{i} - 0.791\hat{j}$	0	0
After Collision 2 (B+C) Frame 84 $t = 2.360\text{s}$				$0.1929\hat{i} - 0.6935\hat{j}$	$-0.2074\hat{i} + 0.9170\hat{j}$	$1.132\hat{k}$	$0.466\hat{i} - 0.791\hat{j}$	$0.5444\hat{i} - 0.2671\hat{j}$	$-0.4737\hat{k}$

**Table 4. Python-Calculated Values Using Point-Mass Simplification.**

	STONE A			STONE B			STONE C		
	$\vec{r}$ (m)	$\vec{v}$ (m/s)	$\vec{\omega}$ (rad/s)	$\vec{r}$ (m)	$\vec{v}$ (m/s)	$\vec{\omega}$ (rad/s)	$\vec{r}$ (m)	$\vec{v}$ (m/s)	$\vec{\omega}$ (rad/s)
Collision 1 (A+B) Frame 53 $t = 1.120\text{s}$	$-0.320\hat{i} + 0.894\hat{j}$	$0.0457\hat{i} - 1.3599\hat{j}$	$0.6586\hat{k}$	$-0.189\hat{i} + 0.629\hat{j}$	0	0			
Post-Collision 1 (A+B) Frame 54 $t = 1.160\text{s}$		$-0.4568\hat{i} - 0.2478\hat{j}$	$2.0433\hat{k}$		$0.5025\hat{i} - 1.0166\hat{j}$	???			
Collision 2 (B+C) Frame 83 $t = 2.320\text{s}$				$0.3768\hat{i} - 0.5150\hat{j}$	$0.5025\hat{i} - 1.0166\hat{j}$	$??\hat{k}$	$0.466\hat{i} - 0.791\hat{j}$	0	0
After Collision 2 (B+C) Frame 84 $t = 2.360\text{s}$				$0.3768\hat{i} - 0.5150\hat{j}$	$-0.04006\hat{i} + 0.09320\hat{j}$	??	$0.466\hat{i} - 0.791\hat{j}$	$0.4681\hat{i} - 0.8466\hat{j}$	$-0.4737\hat{k}$

## VI. Appendix B

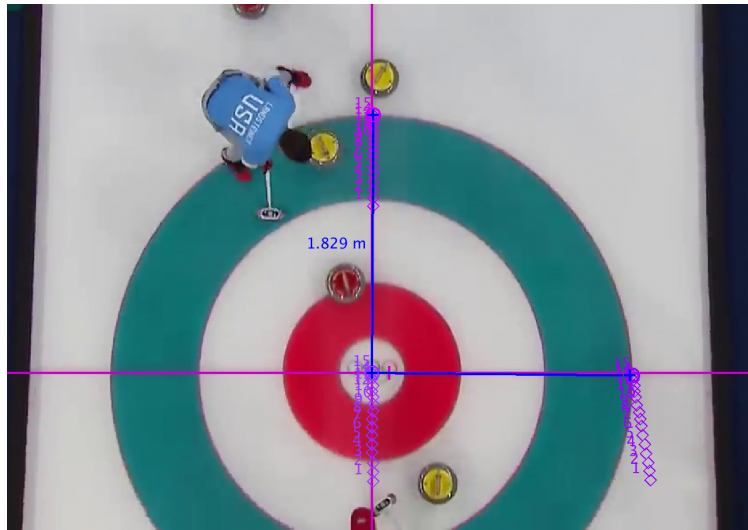


Figure B.1. Configuration of objective axes at the center of circle.

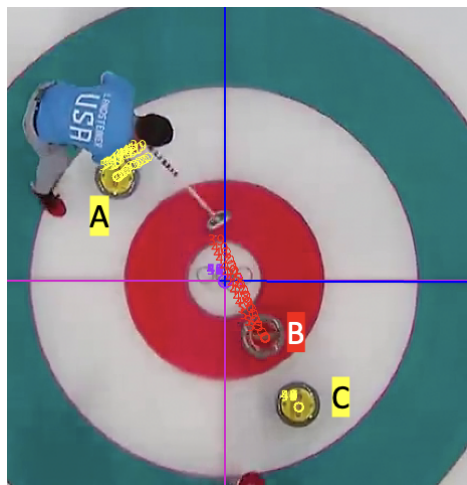
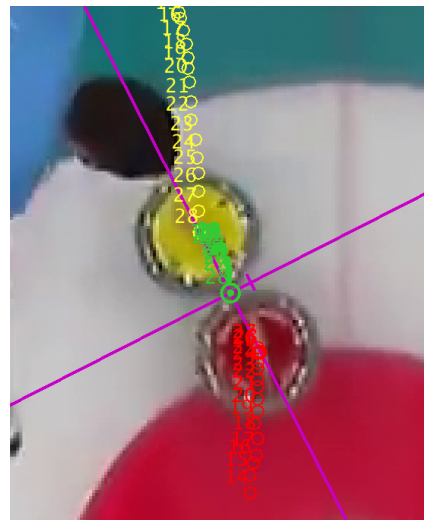


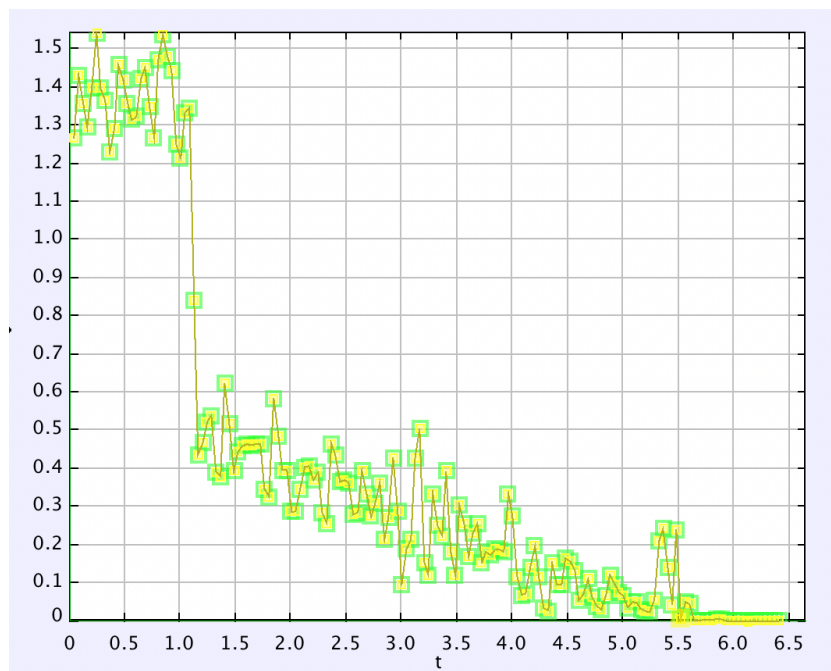
Figure B.2. Denotation of Stones A, B, and C.



Figure B.3. Configuration of centroidal axis and edge-tracking, to find angular motion.



**Figure B.4.** Configuration of normal-tangential axes, centered at the combined COM of two stones, to find coefficient of restitution.



**Figure B.5.** Tracker-generated plot of Stone A's motion. Note that from  $t=1.120\text{s}$  to  $t=5.520\text{s}$ , Stone A decelerates to rest.